

Received October 21, 2017, accepted November 16, 2017, date of publication November 20, 2017, date of current version December 22, 2017.

Digital Object Identifier 10.1109/ACCESS.2017.2775707

# Regulated-Element Frost Beamformer for Vehicular Multimedia Sound Enhancement and Noise Reduction Applications

SUNDAY C. EKPO<sup>1</sup>, (Member, IEEE), BAMIDELE ADEBISI<sup>1</sup>, (Senior Member, IEEE), AND ANDREW WELLS<sup>2</sup>

<sup>1</sup>Department of Electrical and Electronic Engineering, Manchester Metropolitan University, Manchester M1 5GD, U.K.

<sup>2</sup>Department of Research and Development Engineering, Jaguar Land Rover PLC, Warwick CV35 0RR, U.K.

Corresponding author: Sunday C. Ekpo (scekpo@theiet.org)

This work was supported by the Engineering and Materials Science Research Centre, Manchester Metropolitan University, U.K. through the Open Bid Scheme.

**ABSTRACT** A key requirement of an adaptive sensor array involves the ability to deterministically adjust the directional response of the array to reduce noise and reverberations, null interferences, and enhance the gain and recognition of the desired signal. This paper presents a low-carbon adaptive broadband beamforming algorithm called the regulated-element Frost beamformer. It enhances the desired signal based on the noise conditions of the individual omnidirectional sensors deployed in a complex dynamic environment that is prone to steering errors. The investigation of this algorithm was carried out in an interference-dominant, noisy automobile environment characterized by diffuse noise conditions. An embedded system measurement of real-time signals was carried out using omnidirectional acoustic sensors mounted in a model convertible F-Type car driven at speed limits of 20 to 50 mph. The simulation results indicate an array gain enhancement of 2 dB higher than the conventional Frost beamformer and it requires less sensors and filter taps for real-time reconfigurable implementations. The experimental results reveal that the average array gain of the regulated-element beamformer is 2.9 dB higher than the conventional Frost beamformer response. The minimum floor array gain of the regulated-element beamformer is 5 dB, representing 70% noise reduction than the conventional adaptive beamformers.

**INDEX TERMS** Acoustics applications, adaptive beamformer, multimedia infotainment, noise reduction, physical acoustics layer, vehicular noise control.

## I. INTRODUCTION

The reception, recognition and enhancement of acoustic signals in a dynamic complex environment (such as a moving vehicle with multimedia broadband infotainment provisioning) pose a great challenge due to the time-varying nature of the noise sources, reverberations, and interferences impinging on a uniform linear microphone array (ULMA). The literature is replete with system noise evaluation studies spanning handheld cellular devices to space-borne assets involved in data and information communication. Adaptive broadband beamformers have been developed for signal detection and estimation using sensors arrays for numerous applications involving multimedia infotainment, acoustics, communications systems, radar, sonar, seismology, and radio astronomy [1]–[5]. However, the gain enhancement

performance of the conventional adaptive broadband beamformers deteriorates when there is a steering error in the array deployment [6]–[8].

The single-frequency array theories and algorithms are insufficient to address the multimedia acoustic system requirements for wideband operations. The technical challenge relates to designing, developing and deploying the sensor array for a broadband reception of sounds in the presence of uncorrelated noise sources, interferences, and jammers within a moving vehicle [3], [8]–[10]. A number of array-processing applications have been carried out and most of the works assume a farfield source [5] with the signal arriving at the microphone array as plane waves. Furthermore, most practical microphones deployed for in-vehicle multimedia infotainment applications have their

excitation sources situated well within the nearfield [6]. This presents a serious technical constraint in validating the classical farfield assumptions for the beamformer design and has the potential to severely deteriorate the beampattern. The aerodynamic noise dominates at cruising and higher speeds and the system noise characterization usually occurs in the car interior and exterior [1], [3]. At different speed and environmental (such as temperature) conditions, the aerodynamic noise of moving vehicles influences the level of passenger comfort experienced [5], [8]. Hard- and soft-constrained iterative optimization methods have been investigated and proposed for the deterministic and non-deterministic (stochastic) signal processing applications. The majority of the studies have revolved around long and short data runs and the susceptibility of the constrained iterative optimization techniques to cumulative roundoff errors [6]–[11].

To obviate the above problems, we propose the adaptation of the elements of the array for gain computation based on the noise field conditions of individual sensors. The Frost beamformer is a constrained least mean square (LMS) method which is designed to eliminate error accumulation while maintaining a hard constraint. The regulated-element Frost beamforming algorithm (REFBA) adapts noisy sensors to the array performance in real-time (RT) and selectively optimizes the finite impulse response filter taps until the array gain saturates [3]. Furthermore, the REF technique can be implemented as an embedded system with recourse to hardware/software co-design. It constrains array elements with undesirable and corrupting noise, jamming, and interference contents to be screened for the array gain computation. An exclusion principle is applied and accepted after comparing the performance of the array gains involving all the deployed sensors with the array response without the noisy elements. This novel integrated electro-acoustic signal processing technique enables the REF beamformer to have low electronic and acoustic components footprints, resulting in very reliable and cost-effective multimedia infotainment systems manufacturing and implementations.

This paper is organized as follows. Section II provides the system architecture, algorithm, and model analyses of the REFBA. Section III explains the hybrid REF beamformer. Section IV examines the acoustic noise characterization procedure using the REF technique. It states the REF noise model and covers the parameters of the acoustic array system utilized in the aerodynamic noise characterization for a moving vehicle. Beamforming simulations and experiment are explained in section V. Section VI reports the simulation and experimental analysis of the REF noise models for vehicles. Section VII concludes the paper.

## II. REF BEAMFORMER ARCHITECTURE AND MODEL ANALYSIS

### A. SYSTEM ARCHITECTURE

Data-dependent or adaptive beamforming techniques constantly and continuously update their data parameters with

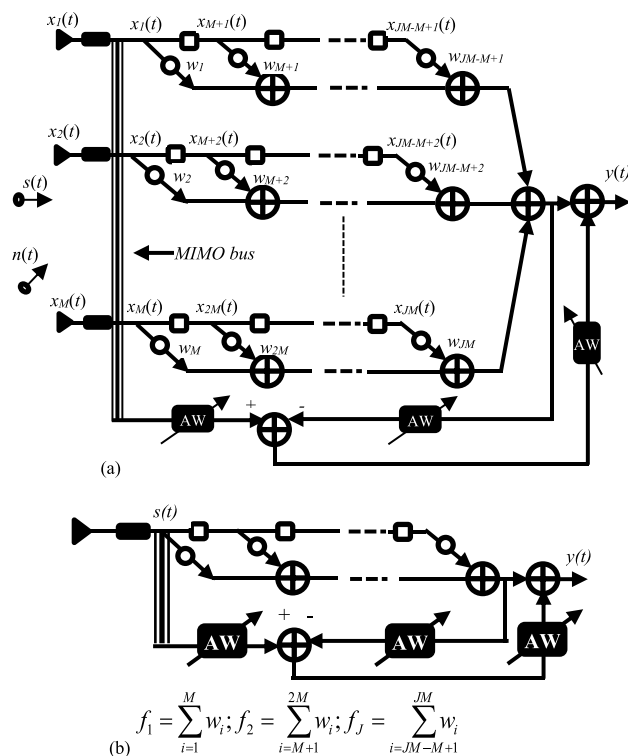


FIGURE 1. System Model Architecture of the REF Beamformer (a) Expanded version (b) Condensed version.

recourse to the received (input) signals. The generic architecture of an adaptive broadband array comprises an array of sensors in tandem with tapped-delay lines and finite impulse response filter networks [13].

The REF beamformer comprises an array of sensors followed by a network of tapped-delay lines, transversal finite impulse response (FIR) filter, and an adjustable element-dependent feedback system. Depending on the noise condition of each sensor, a portion of the received input signal is selectively added to the sum of the filter outputs to yield the feedback outputs. The beamformer output is the sum of the filter and the feedback outputs. The REF beamformer architecture (Fig. 1) contains a multiple-input-multiple-output (MIMO) bus system for selectively adapting the dynamic system noise to the optimal performance requirement of the overall linear array. The REF architecture lends credence to a deterministic tracking of the noise source behavior and parameters for a reliable system-level characterization. Hence, field programmable gates arrays (FPGAs) can be utilized to implement its FIR filter network [3].

### B. SYSTEM MODEL ANALYSIS

The problem formulation of adaptive beamforming methods is a constrained optimization function of the form defined by:

$$\text{minimize } w^T R_{xx} w \quad (1)$$

$$\text{subject to } C^T w = f \quad (2)$$

where  $C$  is the constraint matrix,  $f$ , the constrained system impulse response, and  $R_{XX}$ , the autocorrelation matrix. The sum of the FIR filter outputs gives the output of the Frost beamformer,  $y(t) = w^T x(t)$ . The optimum weight vector,  $w_{opt}$ , for a stationary signal that minimises the expected output power of the array at the time of  $n$ th sample (i.e.,  $E[y^2(n)] = w(n)^T E\{x(n)x^T(n)\}w(n) = w^T E\{x(n)x^T(n)\}w = w^T R_{xx} w$ ), and satisfies the constraint  $C^T w = f$ , has to be derived. This is termed the Wiener solution [12] and the method of Lagrange multiplier is utilised to obtain it as follows:

$$w_{opt} = R_{xx}^{-1} C \left( C^T R_{xx}^{-1} C \right)^{-1} f \quad (3)$$

where the initial weight vector,  $w[0] = f$ . The corresponding system impulse response vector,  $f_{ir}$ , is given by:

$$f_{ir} = C \left( C^T C \right)^{-1} f \quad (4)$$

The regulated-element Frost beamforming algorithm (REFBA) chooses weights to minimise the mean square error between the Frost beamformer output and the reference signal based on an adaptive detection of the received signal at each sensor. Due to the regulated feedback system of the REF beamformer for an optimal noise reduction, the required FIR filter taps is reduced by a factor of two for a 6-dB array gain increase compared with the Frost method. The constraint functions of the REF beamformer can be represented in a matrix form as:

$$W \begin{bmatrix} 1 \\ 1 \\ \cdot \\ \cdot \\ \cdot \\ 1 \end{bmatrix} = \begin{bmatrix} f_1 \\ f_2 \\ \cdot \\ \cdot \\ \cdot \\ f_J \end{bmatrix} \quad (5)$$

where the weight matrix,  $W$ , is given by:

$$W = \begin{bmatrix} w_1 & w_2 & \cdot & \cdot & \cdot & w_M \\ w_{M+1} & w_{M+2} & \cdot & \cdot & \cdot & w_{2M} \\ \cdot & \cdot & & & & \\ \cdot & \cdot & & & & \\ \cdot & \cdot & & & & \\ w_{JM-M+1} & w_{JM-M+2} & & & & w_{JM} \end{bmatrix} \quad (6)$$

and the system impulse response,  $f$ , is obtained as a  $J$ -dimensional vector thus:

$$f = [f_1, f_2, \dots, f_J]^T \quad (7)$$

where  $f_1 = \sum_{i=1}^M w_i, f_2 = \sum_{i=M+1}^{2M} w_i, f_J = \sum_{i=JM-M+1}^{JM} w_i$ .

The noisy signals on taps and the weight vector are represented by  $x(n)$  and  $w$  respectively. The constrained system impulse response,  $f$ , and the matrix of  $JM$  column vectors,  $C$ , are utilized for the constraint formulation. These parameters

are represented as follows:

$$\begin{aligned} x^T(n) &= [x_1(n) \quad x_2(n) \quad \cdot \quad \cdot \quad \cdot \quad x_{JM}(n)], \\ w^T &= [w_1 \quad w_2 \quad \cdot \quad \cdot \quad \cdot \quad w_{JM}], \\ f_{ir}^T &= [f_1 \quad f_2 \quad \cdot \quad \cdot \quad \cdot \quad f_{JM}], \\ C &= [c_1, \quad c_2, \quad \cdot \quad \cdot \quad \cdot, \quad c_J]. \end{aligned}$$

For  $J$  FIR filter coefficients and  $M$  sensors, the entries,  $c_i$ , of the constraint matrix,  $C$ , are the column vectors of length  $JM$  with  $(i - 1)M$  zeros followed by  $M$  ones and  $(J - i)M$  zeros. For a 2-element ULMA system deploying 4 FIR filter taps, the constraint matrix,  $C$ , is given by:

$$C = [c_1, c_2, c_3, c_4]$$

where the entries ( $c_1, c_2, c_3$ , and  $c_4$ ) are obtained as:

$$\begin{aligned} c_1 &= [1 \quad 1 \quad 0 \quad 0 \quad 0 \quad 0 \quad 0 \quad 0] \\ c_2 &= [0 \quad 0 \quad 1 \quad 1 \quad 0 \quad 0 \quad 0 \quad 0] \\ c_3 &= [0 \quad 0 \quad 0 \quad 0 \quad 1 \quad 1 \quad 0 \quad 0] \\ c_4 &= [0 \quad 0 \quad 0 \quad 0 \quad 0 \quad 0 \quad 1 \quad 1] \end{aligned}$$

The expected beamformer output of the individually adaptive regulated-element algorithm can be formulated. The received signal vector,  $S_r(t)$ , for the entire uniform linear array (ULMA) (Fig. 1) is given by:

$$S_r(t) = \sum_{i=1}^M x_i(t) \quad (8)$$

where the received signal at each sensor,  $x_i(t)$ , is given as a function of the received desired signal,  $s_i(t)$ , and dynamic system noise,  $n_i(t)$ , thus:

$$x_i(t) = s_i(t) + n_i(t) \quad (9)$$

The residual noise,  $n'_o$ , is estimated based on the expected (mean average) output signal of the Frost array,  $E[y^2(n)]$ , the received signal at the time of  $n$ th sample,  $S_r(n)$ , and the number of sensors as follows:

$$n'_o(n) = \frac{S_r(n)}{M^M} - ME[y^2(n)] \quad (10)$$

The output of the REF algorithm is obtained by applying sensor-dependent adjustable weight (AW) vectors to the adaptive linear-constrained least mean square architecture output. This is based on the incoming data statistics at each sensor. Mathematically, the array output gain,  $REF_o(n)$ , is obtained (with recourse to Fig. 1) from (1), and (8) to (10) as:

$$\begin{aligned} REF_o(n) &= w^T E[S_r(n)S_r(n)^T]w \\ &+ \frac{S_r(n)}{M^M} - M \left( w^T E[S_r(n)S_r(n)^T]w \right) \quad (11) \\ &M^M \end{aligned}$$

From (11), the REF output at the time of  $n$ th sample can be computed using the following relationship thus:

$$REF_o(n) = \frac{1}{M^{2M}} \left( M^{M+1} (M^{M-1} - 1) w^T E[S_r(n)S_r(n)^T] w + \sum_{i=1}^M x_i(n) \right)$$

or

$$REF_o(n) = \frac{1}{M^{2M}} \left( M^{M+1} (M^{M-1} - 1) w^T R_{xx} w + \sum_{i=1}^M x_i(n) \right) \tag{12}$$

Equation (12) yields a high array gain for an appreciable residual noise reduction. However, the cumulative array signal gain reduces by  $M^{-2M}$  as the number of sensors increases beyond a threshold number. This results in array compression as the active elements are enabled beyond the threshold number. To overcome this challenge, a hybrid regulated-element Frost (HREF) beamformer that improves the residual noise with a corresponding cumulative array gain is discussed in the next section.

### III. HYBRID REF BEAMFORMER

The REF beamformer adjusts the array gain output based on the noise condition of each sensor and its algorithm for the acoustic array system noise modelling has been formulated in the last section by considering the noise properties of individual sensors. The hybrid REF algorithm is derived with the individual array elements enabled for a  $M^{-2}$  feedback threshold factor at the time of the received  $n$ th sample,  $S_r(n)$ .

Given that the expected (mean average) output power of the array is  $E[y^2(n)]$ , the residual noise of the HREF beamformer,  $n'_r$ , is estimated with recourse to Fig 1 and (8) to (10) thus:

$$n'_r(n) = \frac{\sum_{i=1}^M (x_{ri}(n))}{M} - E[y^2(n)] \tag{13}$$

The overall output of the HREF beamformer is obtained by applying element-dependent adjustable weight (AW) vectors based on the incoming data statistics at each ULMA sensor. The output signal is a function of the number sensors and the residual noise extraction estimate for a system noise characterisation. Hence, the HREF beamformer output,  $HREF_o(n)$ , is given by:

$$HREF_o(n) = E(y^2[n]) + \frac{n'_r}{M} \tag{14}$$

or

$$HREF_o(n) = \frac{1}{M^2} \left( M(M-1) E(y^2[n]) + \sum_{i=1}^M (x_{ri}(n)) \right) \tag{15}$$

To incorporate the autocorrelation function and weight vectors into the functional relationship of the array gain, Eq. (6) is modified to compute the HREF beamformer output as follows:

$$HREF_o(n) = \frac{1}{M^2} \left( M(M-1) w^T E[S_r(n)S_r(n)^T] w + \sum_{i=1}^M (x_{ri}(n)) \right)$$

or

$$HREF_o(n) = \frac{1}{M^2} \left( M(M-1) w^T R_{xx} w + \sum_{i=1}^M (x_{ri}(n)) \right) \tag{16}$$

Equations (10) and (13) represent the residual noise extraction functions for the REF and HREF beamformers respectively. The following section explores the procedure that both noise estimating relationships adopt to improve the signal-to-noise ratio of array sensors.

## IV. ACOUSTIC NOISE CHARACTERIZATION

### A. REF NOISE MODELING

An acoustic noise characterization (ANC) in a dynamic system starts with the identification of the noise field condition(s) of individual sensors constituting an acoustic array. In a vehicular environment, the diffuse noise field (DNF) prevails.

Figures 2 and 3 show the adaptive noise cancellation architecture and the acoustic noise modeling flow chart for the REF beamformer respectively.

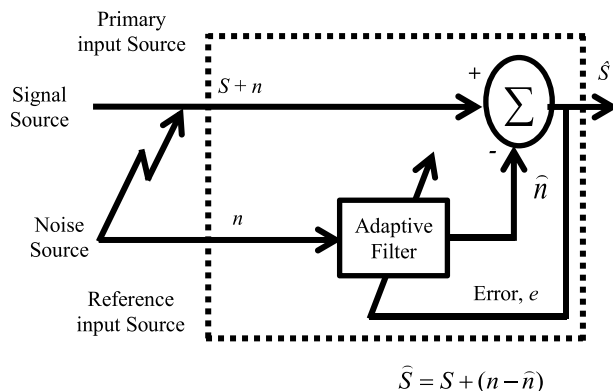


FIGURE 2. Adaptive noise cancellation architecture.

The engine transmission speed and the interaction between the tyre and the road surface generate a noise intensity level that is proportional to the magnitude of the resultant vibration. This translates into a vehicle acoustical discomfort that affects the driver and the passenger in the automobile cabin. Adaptive filters are capable of adjusting their impulse response to filter out the correlated signal in the input. They require no a priori knowledge of the correlated signal in the input [12], [15]. Figure 2 can be implemented to suppress noise contributions in an acoustic array signal processing. The main energy of a car noise pattern is estimated to fall

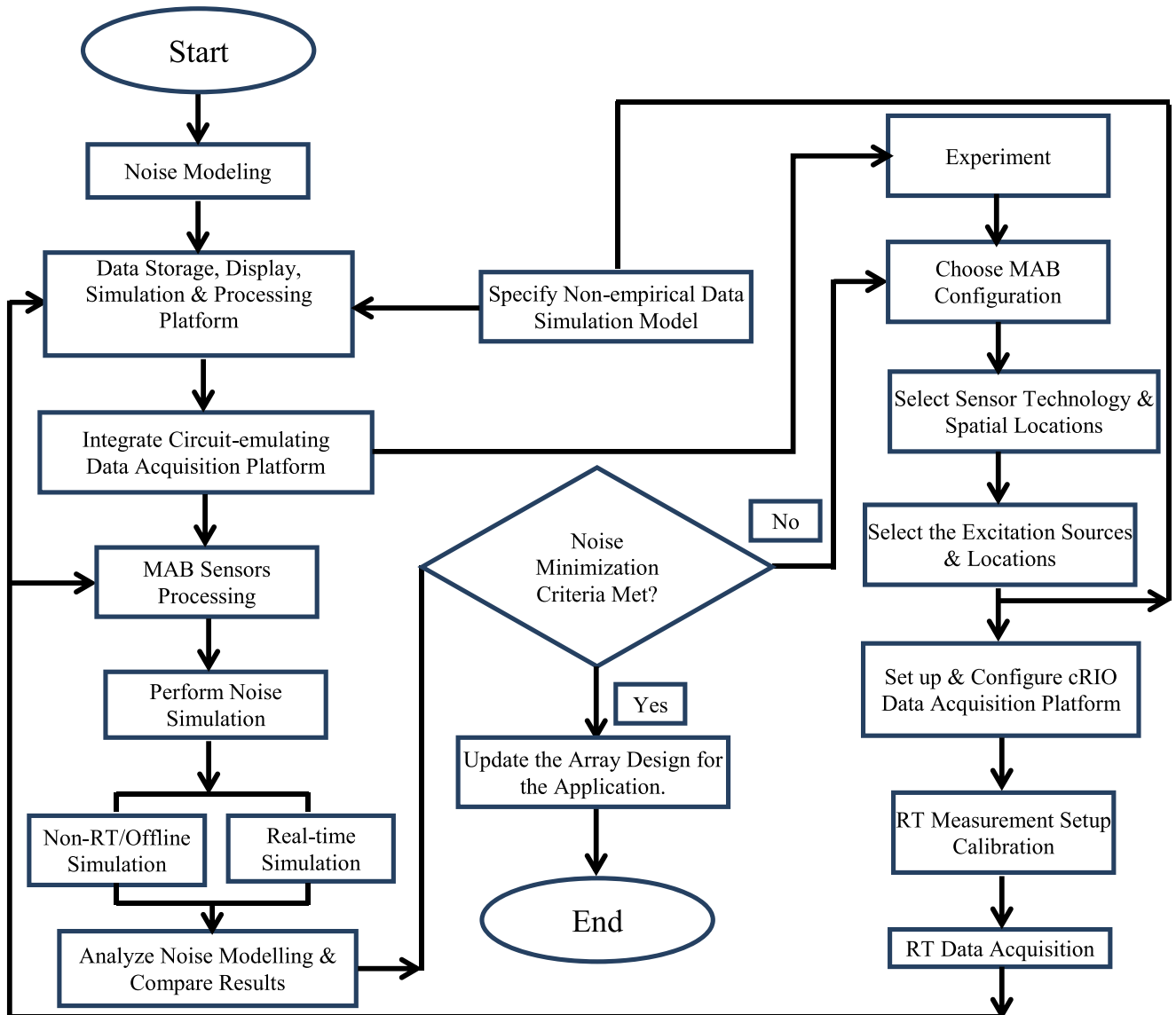


FIGURE 3. Acoustic noise modeling flow chart.

within the frequency range of 5 kHz and below. A number of key factors limit real-time acoustic measurements of moving vehicles. These include background noise, variable vehicle speed (deceleration and acceleration), uncertain vehicle direction, RF/EM interferences, multipath reflections, complicated traffic flow density, sensor differences, and hardware compatibility constraints. Vehicle speed and changes in direction determine the frequency component shift in the moving object signal. The REF beamformer considers these real-time sound validation constraints while implementing the residual noise extraction algorithm on the complex dynamic system.

### B. REF NOISE CHARACTERIZATION PROCEDURE

The noise characterisation procedure of the REF beamformer comprises two paths: the non-empirical and the empirical validations. The non-empirical ANC procedure path involves a system model simulation based on a historical database. Similarly, the empirical ANC procedure path

entails an experimental measurement based on a real-time data acquisition. The noise modelling procedure is illustrated in Fig. 3. The simulation process path is meant for a non-RT, offline and hypothetical data-generation validation of the system noise model. The development computer runs the appropriate software packages including a real-time operating system for a compact real-time input/output (cRIO), CAD programs and graphical, object-oriented and technical simulation/computing softwares. A system noise estimating relationship (SNER) based on the non-empirical data acquired is obtained from a statistical analysis and curve-fitting implementation.

## V. BEAMFORMING SIMULATION AND EXPERIMENT

### A. ANALYSES OF TIME DELAY, FROST AND REF BEAMFORMERS

The simulations and experimental investigation of the time delay, Frost, and REF beamformers were carried out to

extract desired speech signals in an interference-dominant, noisy environment such as the one found in an automobile characterized by diffuse noise conditions. The routes were carefully mapped to enable the noise signals to be obtained at the worst traffic conditions. Noise waveforms and spectra at car speed limits of 20 mph, 30 mph, 40 mph, and 50 mph were measured using omnidirectional MEMS acoustic sensors mounted inside a closed-roof car. Multichannel signals received by the microphone array were simulated by loading two recorded speeches, vehicle noise recordings at the considered speed limits, and one laughter recording; the laughter audio segment was loaded as an interference signal arriving at 20° azimuth and 0° elevation angles. The sampling frequency of the acoustic signals was set to 8 kHz. The incident azimuth and elevation directions of the first speech signal were maintained at ±90°. The direction of the second speech signal was at -10° azimuth, and 10 elevation angles. The signal-to-interference-and-noise ratio (SINR) gain for the ULMA system was determined for the Frost and REF methods. Table 1 shows a summary of the array performance results for the time delay, Frost, and REF beamformers. It is obvious that the FBA is outperformed by the REFBA by over 1.6 W output power (2 dB gain). The hybrid REF indicates approximately 1.8 W received power (2.5 dB gain) better than the Frost beamformer. The REFBA reveals a signal-to-noise ratio (SNR)-based steering gain enhancement of over 3 W received power (5 dB) more than the FBA output in the incident angle (-30, 0) direction. The REF technique responses also indicate the capability of the algorithm to perform real-time reconfiguration of audio processing and correct system-level hardware anomalies in the presence of steering errors.

TABLE 1. Array performance results for the case study beamformers.

| No. of Acoustic Sensors: |       | 2                      |       |       |       |       |       |       |
|--------------------------|-------|------------------------|-------|-------|-------|-------|-------|-------|
|                          |       | Microphone Spacing (m) |       |       |       |       |       |       |
|                          |       | 0.05                   | 0.10  | 0.15  | 0.20  |       |       |       |
| MAB Technique            |       | Array Gain (dB)        |       |       |       |       |       |       |
| TD                       | 1.49  | 3.76                   | 5.78  | 5.26  |       |       |       |       |
| Frost                    | 8.23  | 8.85                   | 8.52  | 7.93  |       |       |       |       |
| REF                      | 10.28 | 10.79                  | 10.89 | 10.96 |       |       |       |       |
| Sensor Spacing (m)       |       | 0.05                   |       |       |       |       |       |       |
|                          |       | Number of Microphones  |       |       |       |       |       |       |
|                          |       | 2                      | 4     | 6     | 8     |       |       |       |
| MAB Technique            |       | Array Gain (dB)        |       |       |       |       |       |       |
| TD                       | 1.49  | 4.34                   | 7.07  | 8.50  | 3.76  | 8.17  | 10.06 | 11.36 |
| Frost                    | 8.23  | 10.37                  | 12.08 | 13.61 | 8.85  | 12.11 | 14.72 | 16.29 |
| REF                      | 10.28 | 10.50                  | 12.08 | 13.61 | 10.79 | 12.23 | 14.72 | 16.29 |

The REF and Frost beamformers have been utilized to investigate the array gain enhancement and speech recognition profile of a moving vehicle at different speeds. The dominant noise components at different vehical speeds include motor noise, acceleration, and tyre/road noise. Table 2 states the minimum and maximum acoustic array gains of a moving vehicle for the Frost, REF and HREF beamformers. With reference to a 1-W input power, the Frost beamformer gives an average minimum array signal power output of approximately 1.1 W compared with the REF’s 2.6 W, and hybrid

TABLE 2. Array gain at different vehicle speeds.

| Speed (mph) | LimitArray Gain (dB) |      |      |      |            |      |
|-------------|----------------------|------|------|------|------------|------|
|             | Frost                |      | REF  |      | Hybrid REF |      |
|             | Min                  | Max  | Min  | Max  | Min        | Max  |
| 20          | 18.4                 | 23.2 | 22.3 | 26.4 | 23.5       | 27.2 |
| 30          | 18.5                 | 24.1 | 22.5 | 27.0 | 23.9       | 28.2 |
| 40          | 17.5                 | 21.4 | 21.5 | 24.9 | 23.0       | 26.3 |
| 50          | 19.0                 | 27.3 | 23.0 | 29.3 | 24.3       | 29.6 |

REF’s 3.8 W. Similarly, the average maximum array signal powers for the Frost, REF, and hybrid REF are approximately 8 W (Fig. 4), 12 W (Fig. 5), and 13 W (Fig. 6) respectively over the case study speed limits. The array gain difference is approximately 3 dB at any given moving vehicle speed.

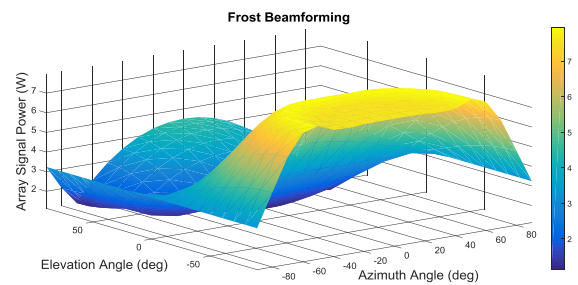


FIGURE 4. FBA (d = 10 cm; 2-element ULMA; FIRL = 5).

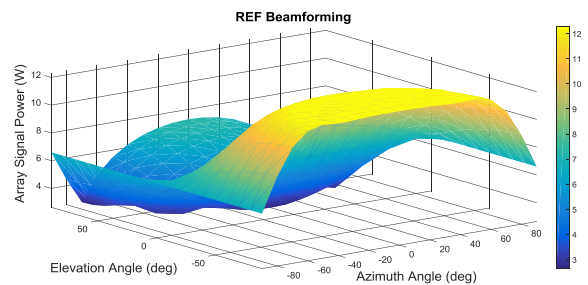


FIGURE 5. REFBA (d = 10 cm; 2-element ULMA; FIRL = 5).

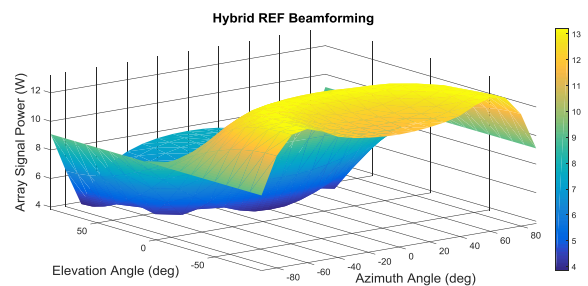


FIGURE 6. Hybrid REFBA (d = 10 cm; 2-element ULMA; FIRL = 5).

VI. REF NOISE SIMULATION AND EXPERIMENTAL ANALYSIS

A simulation of the noise extraction of the REF noise model was carried out with recourse to the signal sources, noise field

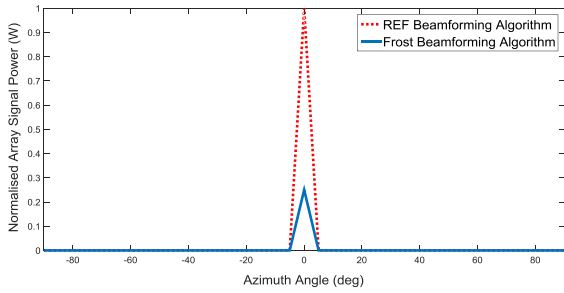


FIGURE 7. Broadside Array Signal Power for the ULMA ( $N = 2$ ;  $d = 10$  cm; Filter Length = 2).

condition(s), number of sensors, upper frequency aliasing threshold (which sets the element spacing), and the filter taps required. In the experimental investigation of the REF noise model for vehicles, we considered the prevailing automobile speed limits in the UK. The routes were carefully mapped to enable the noise signals at car speed limits of 20 mph, 30 mph, 40 mph and 50 mph to be measured using omnidirectional MEMS acoustic sensors.

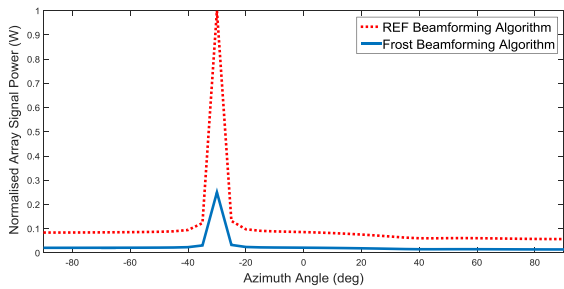


FIGURE 8. SNR-based Steering Signal Power for the FBA and REFBA ( $N = 2$ ;  $d = 10$  cm; Filter Length = 2).

A. RESULTS AND DISCUSSION

In Fig. 7, the REF achieves a broadside array signal power enhancement of approximately four times better than the Frost algorithm. Furthermore, the SNR-based steering gain (Fig. 8) for the REFBA ULMA reveals a gain enhancement of over 5 dB more than the FBA output in the incident angle (-30, 0) direction. The normalised broadside system selectivity response for the REFBA (Incident Angle = (0, 0)) is approximately 5 dB better than the FBA response. The SNR-based dynamic system selectivity gains of the ULMA based on the residual noise extraction technique was also investigated; the REF outperforms the conventional Frost beamformer by 3 dB. The results indicate that fewer filter taps are required for the REFBA compared with the FBA resulting in a lower computational cost than the latter. Since one needs to invert a 4-by-2 matrix, the REFBA offers a less expensive real-time processing using a field programmable gates array (FPGA)-based embedded signal conditioning system. Table 3 shows an analysis of the Doppler noise power of a moving vehicle at different source excitation frequencies and car speeds. The REF algorithm analysis shows that the reported

TABLE 3. Doppler noise power at different vehicle speeds.

| Source Frequency (Hz) | Vehicle Speed (mph)       |         |         |         |         |         |         |
|-----------------------|---------------------------|---------|---------|---------|---------|---------|---------|
|                       | 20                        | 30      | 40      | 50      | 60      | 70      | 80      |
|                       | Doppler Noise Power (dBm) |         |         |         |         |         |         |
| 3000                  | -139.10                   | -139.04 | -138.99 | -138.94 | -138.88 | -138.83 | -138.78 |
| 2000                  | -140.86                   | -140.80 | -140.75 | -140.70 | -140.64 | -140.59 | -140.54 |
| 1500                  | -142.11                   | -142.05 | -142.00 | -141.95 | -141.89 | -141.84 | -141.79 |
| 1000                  | -143.87                   | -143.81 | -143.76 | -143.71 | -143.65 | -143.60 | -143.55 |
| 500                   | -146.88                   | -146.82 | -146.77 | -146.72 | -146.66 | -146.61 | -146.56 |
| 440                   | -147.43                   | -147.38 | -147.32 | -147.27 | -147.22 | -147.17 | -147.12 |

adaptive beamformer can accurately estimate the Doppler frequency for applications involving satellite navigation system receivers of vehicles under varying environmental conditions.

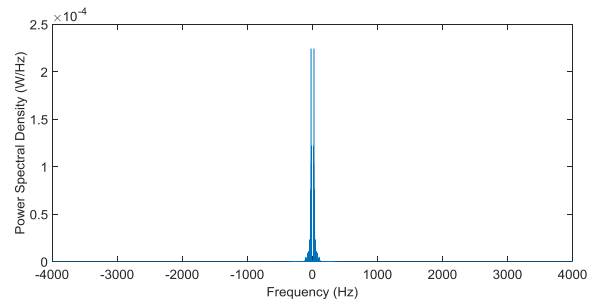


FIGURE 9. Periodogram Power Spectral Density of a Car Noise at 20 mph.

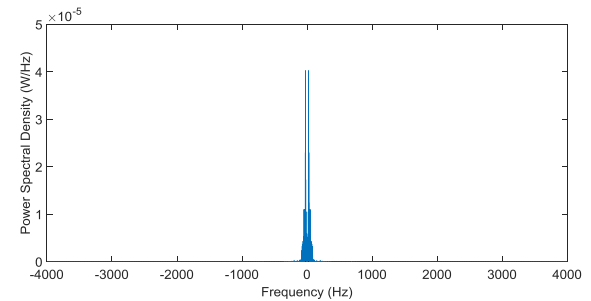


FIGURE 10. Periodogram Power Spectral Density of a Car Noise at 30 mph.

Figures 9 and 10 depict the double-sided periodogram noise power spectrum estimates of the case study moving car at the speed limits of 20 mph, 30 mph, 40 mph, and 50 mph respectively. The average noise power for the considered speed limits is approximately -60 dB from about 0.2 to 3 kHz. At a speed limit of 20 mph, the noise power shows a more compact frequency response with a maximum value of -40 dB at close to DC level and about -120 dB at 4 kHz. A similar response is observed at 30 mph, 40 mph, and 50 mph except for the obvious lower noise power (< -140 dB) at the 1.5 to 2.5 kHz spectral contents.

Table 4 shows the measured noise power and signal-to-noise ratio (SNR) of a moving vehicle at different speed limits. The SNR of the Frost beamforming technique trails

**TABLE 4. Measured noise power and SNR at different vehicle speeds.**

| Speed Limit (mph) | Noise Power (dB) |        | SNR (dB) |       |
|-------------------|------------------|--------|----------|-------|
|                   | 1.715 kHz        | Total  | Frost    | REF   |
| 20                | -142.8           | -30.27 | 63.78    | 66.10 |
| 30                | -135.0           | -34.45 | 67.96    | 72.19 |
| 40                | -125.9           | -28.81 | 61.40    | 64.40 |
| 50                | -128.5           | -36.64 | 70.06    | 75.01 |

behind the REF algorithm by approximately 3-dB and 4-dB margins for even and odd speed limits respectively. The total system noise is nonlinear with 40 mph giving the highest noise power and 50 mph, the lowest noise power. This is due to the dynamics of the system where the acoustic sensors are deployed at the time. The extracted residual noise power (ERNP) for both acoustic sensors averages at approximately 31 W (i.e., 15 dBW). Table 5 shows that the prevailing noise field condition affects the amount of residual noise that can be extracted within a complex dynamic system. Moreover, by using an acoustic array design, the moving vehicle system noise can be characterised accurately and reduced systematically for a predetermined passenger comfort.

**TABLE 5. Extracted residual noise power at different vehicle speeds.**

| Speed Limit (mph) | ERNP (dB) |          |
|-------------------|-----------|----------|
|                   | Sensor 1  | Sensor 2 |
| 20                | 15.2013   | 15.2014  |
| 30                | 15.1688   | 15.1688  |
| 40                | 14.6923   | 14.6908  |
| 50                | 15.0752   | 15.0760  |

## B. POTENTIAL APPLICATIONS OF THE REF BEAMFORMER

The expanding city-wide traffic congestion problem can be improved through an intelligent deployment of REF beamformer sensors for an event-driven vehicular access control strategy implementation. The current trend is that of an increasing number of vehicular communication sensors and onboard compute power to process the received big data [13]. The REF beamformer also has the potential to enhance passive cooperative collision warning [14] for reliable vehicular safety messaging via electro-vibro-acoustic emissions. This is utilised to achieve a highly reliable real-time collision avoidance system. Due to the steerable nature of the REF beamformer sensors array, different channel models, vehicular densities, transmission frequencies, and predictive handovers can be implemented concurrently [14]. Another potential application for the REF beamformer is in capability-based small satellite [19] data transmission. The REF beamformer has the capability to enable low computational burden by global navigation satellite system receivers [15]–[17] that require the implementation of low-complexity algorithms for on-demand real-time and sensor array signal processing. Given the size, weight and power limitations of small satellites, the REF technique would provide a cost-effective and low-power solution to onboard signal processing

for high data link margins and space-borne smart earth observation applications. Furthermore, hidden parametric and non-parametric sound quality agreement can be reliably assessed using adaptive beamforming techniques. The experimental measurements and simulation models presented in this paper show that at even speed limits (including 20 mph and 40 mph), the corresponding SNR of the REF beamformer averages at 65 dB. This result shows an appreciable agreement with the acoustic noise response of electric powertrains modeled using the boundary element method [18] over the same operating frequencies at vehicular speed limits. Hence, this indicates a potential application for the multiphysics modeling of electric powertrains [19], [20]. The proposed REF technique for the sound enhancement and noise characterization of complex dynamic system uses fewer computational resources than the state-of-the-art beamformers. Hence, this promises a low-power, low-component footprint and cost-effective electro-acoustic system characterization.

## VII. CONCLUSION

The regulated-element Frost beamformer is an adaptive algorithm that selectively enhances the desired signal based on the noise field conditions in a dynamic complex environment. This algorithm was utilized to investigate the effect of different vehicle speeds on an acoustic array gain in real-time. The dynamic system selectivity gains of the array based on the residual noise extraction technique revealed that the regulated-element Frost outperforms the conventional Frost beamformer by 3 dB. The broadside signal-to-noise ratio-based array gain for the regulated-element Frost beamformer is at least four times the value of the conventional Frost beamformer for each threshold frequency. The steering error-correcting capability of the algorithm makes it suitable for real-time recognition and enhancement of signals without a priori knowledge of their properties. The REF algorithm requires fewer finite impulse response filters (FIR) than the traditional adaptive beamforming techniques. Thus, the algorithm has a low complexity and converges faster than its competing methods.

Moreover, various electronic communication applications can be implemented with the presented adaptive beamformer (including advanced smart sensors signaling and internet of things networking; predictive collision warning; adaptive moving vehicle high-speed wireless handover; inter-vehicle trustworthiness estimation; efficient wireless power transfer; and reconfigurable inter-satellite data transmission).

## REFERENCES

- [1] I. Tashev, M. Seltzer, Y.-C. Ju, Y. Wang, and A. Acero, "Commute UX: Voice enabled in-car infotainment system," in *Proc. Mobile HCI*, 2009, pp. 1–7.
- [2] S. Ekpo, B. Adebisi, A. Sabagh, and A. Wells, "Gain enhancement of acoustic beamforming arrays in complex dynamic systems," in *Proc. 30th Annu. Rev. Prog. Appl. Comput. Electromagn.*, Jacksonville, FL, USA, Mar. 2014, pp. 720–725.
- [3] M. Omologo, "Front-end processing of a distant-talking speech interface for control of an interactive TV system," *J. Acoust. Soc. Amer.*, vol. 123, no. 5, p. 3181, 2008.



- [4] B. Adebisi, S. Ekpo, A. Sabagh, and A. Wells, "Acoustic noise characterisation in dynamic systems using an embedded measurement platform," in *Proc. 30th Annu. Rev. Progr. ACES*, Jacksonville, FL, USA, 2014, pp. 726–731.
- [5] M. Strupl and P. Sovka, "Analysis and simulation of Frost's beamformer," *Radioengineering*, vol. 12, no. 2, pp. 1–9, 2003.
- [6] S.-J. Chern and C.-Y. Sung, "The hybrid Frost's beamforming algorithm for multiple jammers suppression," *Signal Process.*, vol. 43, no. 2, pp. 113–127, 1995.
- [7] B. Adebisi, S. C. Ekpo, A. Sabagh, and A. Wells, "Acoustic signal gain enhancement and speech recognition improvement in smartphones using the REF beamforming algorithm," in *Proc. 9th IEEE/IET Int. Symp. Commun. Syst., Netw. Digit. Signal Process.*, Manchester, U.K., Jul. 2014, pp. 472–477.
- [8] S. Doclo and M. Moonen, "Superdirective beamforming robust against microphone mismatch," *IEEE Trans. Audio, Speech, Language Process.*, vol. 15, no. 2, pp. 617–631, Feb. 2007.
- [9] J. Meyer and G. W. Elko, "Exploring spherical microphone arrays for room acoustic analysis," *J. Acoust. Soc. Amer.*, vol. 131, no. 4, p. 3208, 2012.
- [10] Y. Sun, J. Zhang, and X. Yang, "Design of experimental adaptive beamforming system utilizing microphone array," in *Proc. IET Int. Radar Conf.*, Xi'an, China, Apr. 2013, pp. 1–5.
- [11] H. Duan, B. P. Ng, C. M. S. See, and J. Fang, "Broadband beamforming using TDL-form IIR filters," *IEEE Trans. Signal Process.*, vol. 55, no. 3, pp. 990–1001, Mar. 2007.
- [12] J. Benesty, J. Chen, and Y. A. Huang, "Study of the widely linear Wiener filter for noise reduction," in *Proc. IEEE Int. Conf. Acoust. Speech Signal Process. (ICASSP)*, Mar. 2010, pp. 205–208.
- [13] R. Florin and S. Olariu, "A survey of vehicular communications for traffic signal optimization," *Veh. Commun.*, vol. 2, no. 2, pp. 70–79, 2015.
- [14] N. Jaber, W. G. Cassidy, K. E. Tepe, and E. Abdel-Raheem, "Passive cooperative collision warning (PCCW) MAC designs for reliable vehicular safety messaging," *Veh. Commun.*, vol. 2, no. 2, pp. 95–109, 2015.
- [15] S. C. Ekpo and D. George, "A system engineering analysis of highly adaptive small satellites," *IEEE Syst. J.*, vol. 7, no. 4, pp. 642–648, Dec. 2013.
- [16] N. Linty and L. L. Presti, "Doppler frequency estimation in GNSS receivers based on double FFT," *IEEE Trans. Veh. Technol.*, vol. 65, no. 2, pp. 509–523, Feb. 2016.
- [17] S. C. Ekpo and D. George, "Impact of noise figure on a satellite link performance," *IEEE Commun. Lett.*, vol. 15, no. 9, pp. 977–979, Sep. 2011.
- [18] C. Ma, Q. Li, L. Deng, C. Chen, Q. Liu, and H. Gao, "A novel sound quality evaluation method of the diagnosis of abnormal noise in interior permanent-magnet synchronous motors for electric vehicles," *IEEE Trans. Ind. Electron.*, vol. 64, no. 5, pp. 3883–3891, May 2017.
- [19] Y. Fang and T. Zhang, "Sound quality investigation and improvement of an electric powertrain for electric vehicles," *IEEE Trans. Ind. Electron.*, to be published, doi: [10.1109/TIE.2017.2736481](https://doi.org/10.1109/TIE.2017.2736481).
- [20] J. Le Besnerais *et al.*, "Multiphysics modeling: Electro-vibro-acoustics and heat transfer of PWM-fed induction machines," *IEEE Trans. Ind. Electron.*, vol. 57, no. 4, pp. 1279–1287, Apr. 2010.



**SUNDAY C. EKPO** (M'08) received the M.Sc. degree in communication engineering and the Ph.D. degree in electrical and electronic engineering from the University of Manchester, Manchester, U.K., in 2008 and 2011, respectively. He is currently a Lecturer in electrical and electronic engineering with the Manchester Metropolitan University, U.K. His specialty spans adaptive satellite system design, multiphysics characterization of RF and optical transceivers, multiobjective system engineering, intelligent sensors design, and Internet of Things implementations. He is a member of the IET, U.K., the AIAA, USA, and the Applied Computational Electromagnetics Society, USA and a fellow of the Higher Education Academy, U.K.



**BAMIDELE ADEBISI** (SM'06–M'09–SM'15) received the bachelor's degree in electrical engineering from Ahmadu Bello University, Zaria, Nigeria, in 1999, and the master's degree in advanced mobile communication engineering, and the Ph.D. degree in communication systems from Lancaster University, U.K., in 2003 and 2009, respectively. He was a Senior Research Associate with the School of Computing and Communication, Lancaster University, from 2005 to 2012.

He joined Metropolitan University, Manchester, in 2012, where he is currently a Reader with Communication Systems and the Director of the EMS Research Centre. He is currently a Chartered Engineer, a member of the IET. He is particularly interested in research and development of communication technologies for electrical energy monitoring/management, transport, water, critical infrastructures protection, home automation, Internet of Things, and Cyber Physical Systems. He has several publications in the research area of data communications over power line networks and smart grid.



**ANDREW WELLS** received the master's degree in mobile communications and the Ph.D. degree in communications system and computer science from Lancaster University, U.K., in 2007 and 2010, respectively. In 2011, he joined the Advanced Electrical Research Department with Jaguar Land Rover (JLR) involved in several projects focusing on the development of future infotainment and vehicle connectivity. He joined the Electrical and Electronic Software Engineering

Department, JLR and is currently the Technical Lead for JLRs cross-carline next generation audio platform. He is particularly interested in the research and development of communications technologies for vehicle communications (V-X), Internet of Things, autonomous vehicles, and automotive security.

...